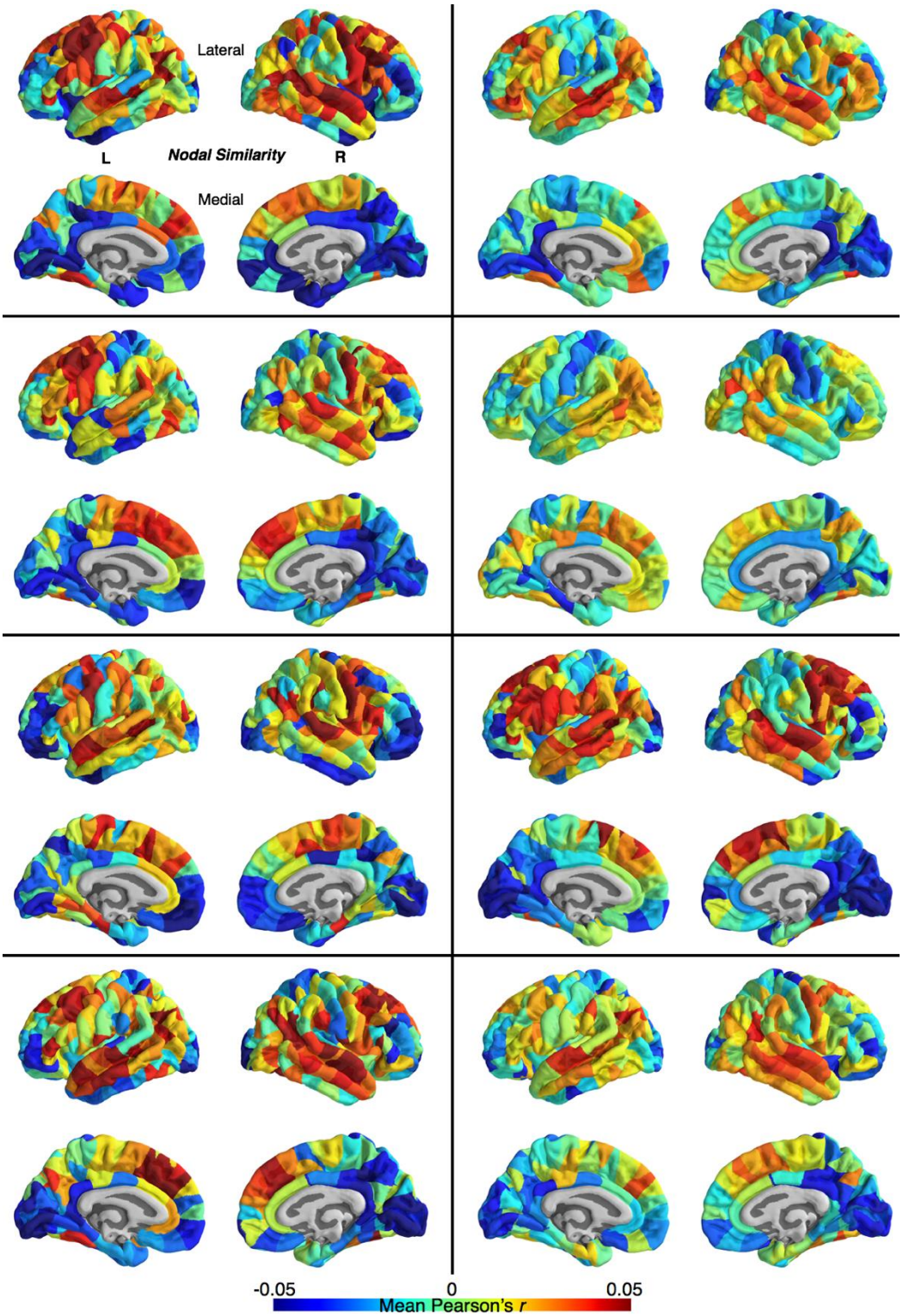

Figure S1. Example individual multi-modal morphometric similarity maps from the primary (NSPN) cohort, Related to Figure 2. The average edge strength of the multimodal (10-feature) morphometric similarity matrices is plotted on a standard (fsaverage) template surface for eight subjects. Although the topography of nodal similarity is unique to the individual, the pattern generally follows a stereotyped distribution, with regions of high similarity being found in association cortical areas and regions with low similarity being found in primary somatosensory and visual cortical areas.

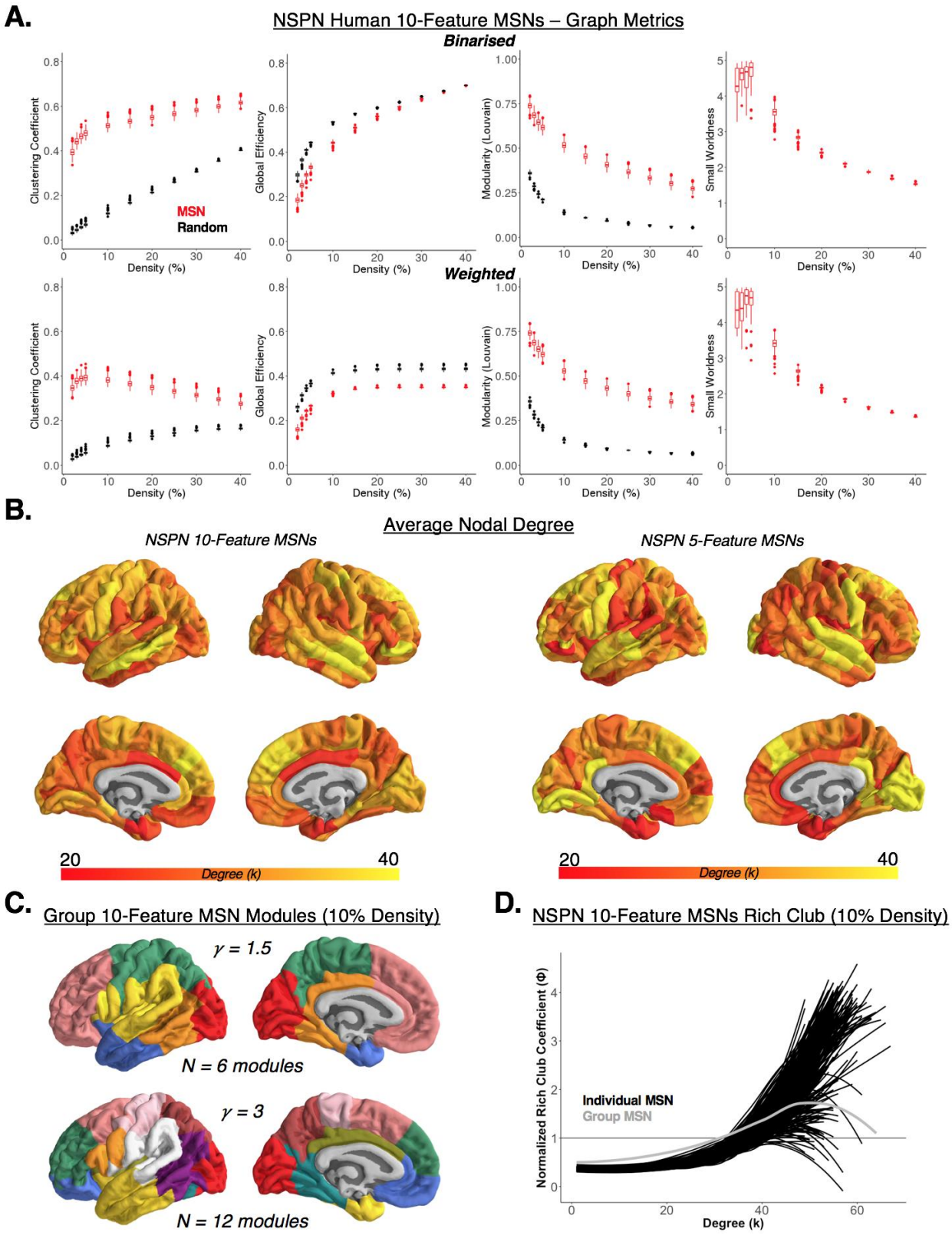

Figure S2. Topological properties of the MSNs in the primary (NSPN) cohort, Related to Figure 2. A) Network properties, including the clustering coefficient, global efficiency, modularity, and small-world coefficient were computed for the individual 10-feature multimodal NSPN MSNs (red) compared to random

networks (black), at varying connection densities (2%, 3%, 4%, and 5-40%, 5% intervals). Random networks were generated by preserving the same number of nodes and edges as each respective individual MSN. Both the binarised and weighted MSNs, like many other brain networks, possess a small-world topology with high modularity. **B)** Nodal degree (i.e., the sum of the number of supra-thresholded edges for each node) was calculated for the individual MSNs, each thresholded at 10% connection density. Plots show nodal degree values averaged across subjects. Across subjects, nodal degree was similar for the 10-feature (Left) and 5-feature (Right) MSNs (median r = 0.37, range = 0.33-0.38, all P < 0.001), with high-degree hubs generally being located in association cortical areas. **C)** Plots of two modular decompositions (yielding N=6 and N=12 modules) of the group average 10-feature multimodal MSN. We observed a hierarchical structure of modules, with the 4-module solution (see Figure 2) being sub-parcellated in an anatomically-relevant manner. For example, the temporal (green) module in Figure 2 is broken into constituent posterior (orange), anterior (blue), and superior (yellow) sections in the 6-module solution. **D)** Normalised rich club curves calculated for each individual MSN, as well as the group average 10-feature multimodal MSN (each thresholded at 10% connection density), showing the existence of a rich club. The rich club coefficient (Φ) is a measure of how inter-connected hubs are relative to connections with non-hubs, at varying thresholds of degree. The normalised rich club coefficient is calculated as the ratio of the empirical coefficient to the coefficient of a random network, and thus the rich club of the empirical network can be defined at the value of k where Φ is greater than 1.

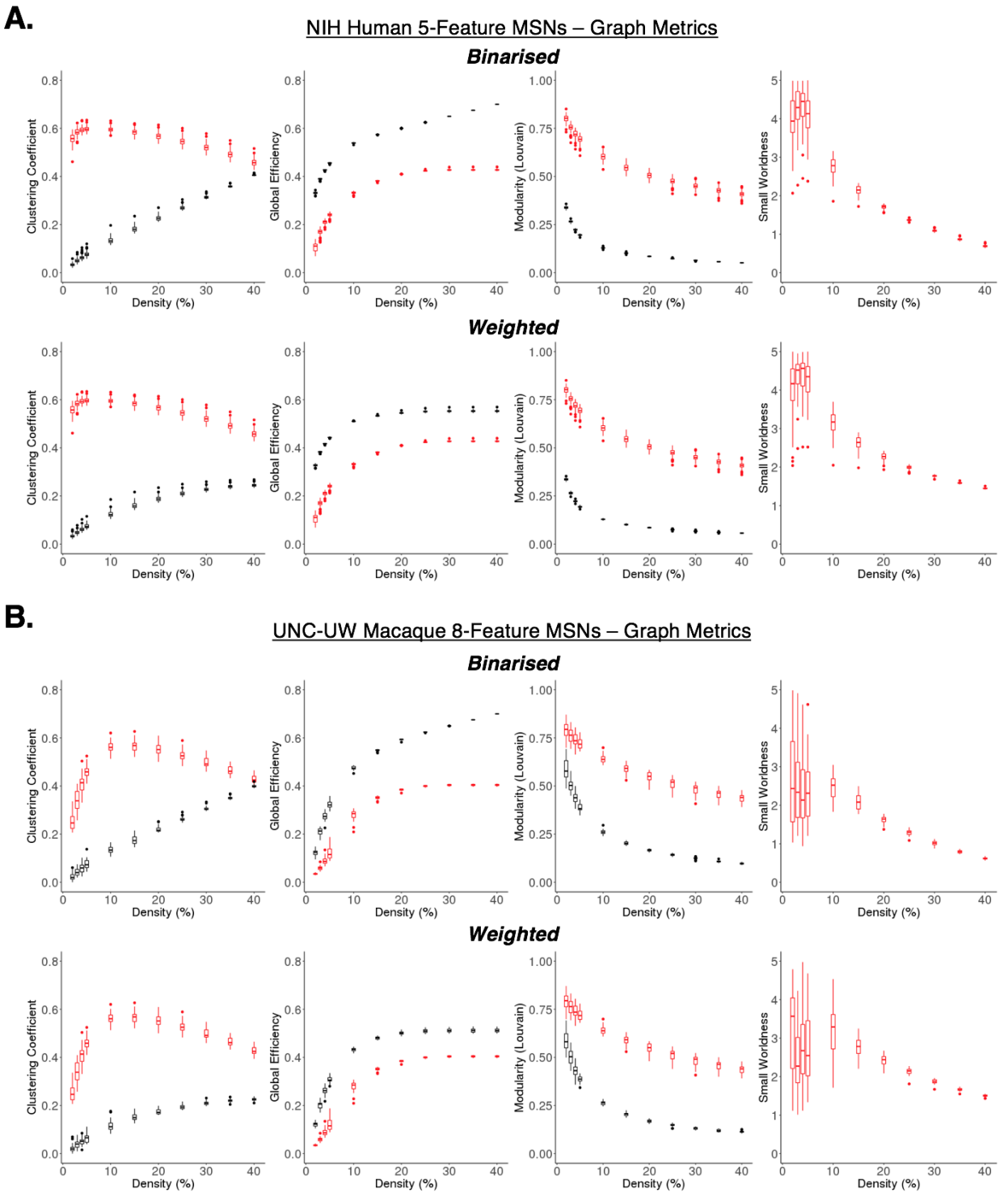

Figure S3. Topological properties of the MSNs from the NIH T1w human and UNC-UW macaque cohorts, Related to Figure 2. The network properties for an independent normative human (A) and macaque cohort (B), estimated as in Figure S2, were highly consistent with those found in the MSNs in the primary NSPN cohort (i.e., small-world with high modularity). These results demonstrate the reproducibility and generalisability of morphometric similarity mapping using data acquired at different field strengths and processed with different analysis pipelines and software.

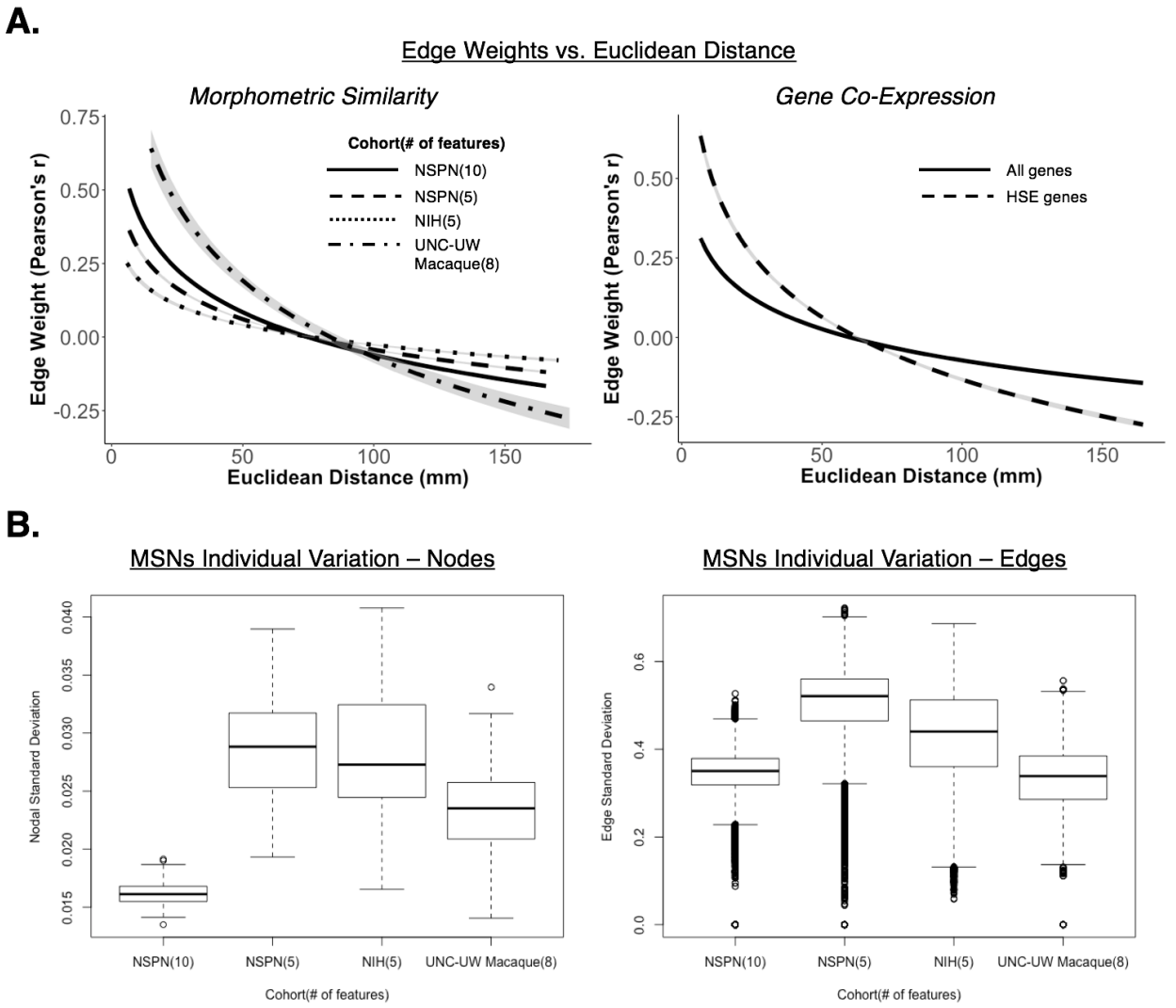

Figure S4. Distance effects on edge weights, and assessment of inter-individual variation in the MSNs, Related to Figures 2 and 4. A) Logarithmic regression curves showing the effect of distance on the edge weights of each of the group average MSNs (Left) and the whole-genome (N = 20,737 genes) and HSE-only (N = 19 genes) gene co-expression networks (Right). For all networks, long distance connections were generally weaker than short distance connections. The distance of each edge for the group macaque MSN was scaled by a factor of three to account for brain size differences between the species. **B)** Boxplots showing inter-individual variation of the MSNs of each cohort, assessed as the standard deviation across subjects for each of the edges (Right) and nodal averages of the edge weights (Left). At the level of the nodes, the 5-feature T1w MSNs had a larger average standard deviation than the 10-feature multimodal human and 8-feature multimodal macaque MSNs, as expected given the fewer amount of features used to generate the networks. At the level of the edges, the trend was similar, however the multimodal macaque MSNs exhibited a lower average standard deviation (albeit a wider range) than the multimodal 10-feature multimodal human MSNs. Lower and upper bounds of the boxplots represent the 1st (25%) and 3rd (75%) quartiles, respectively. Confidence intervals in A) represent the standard error of the mean.

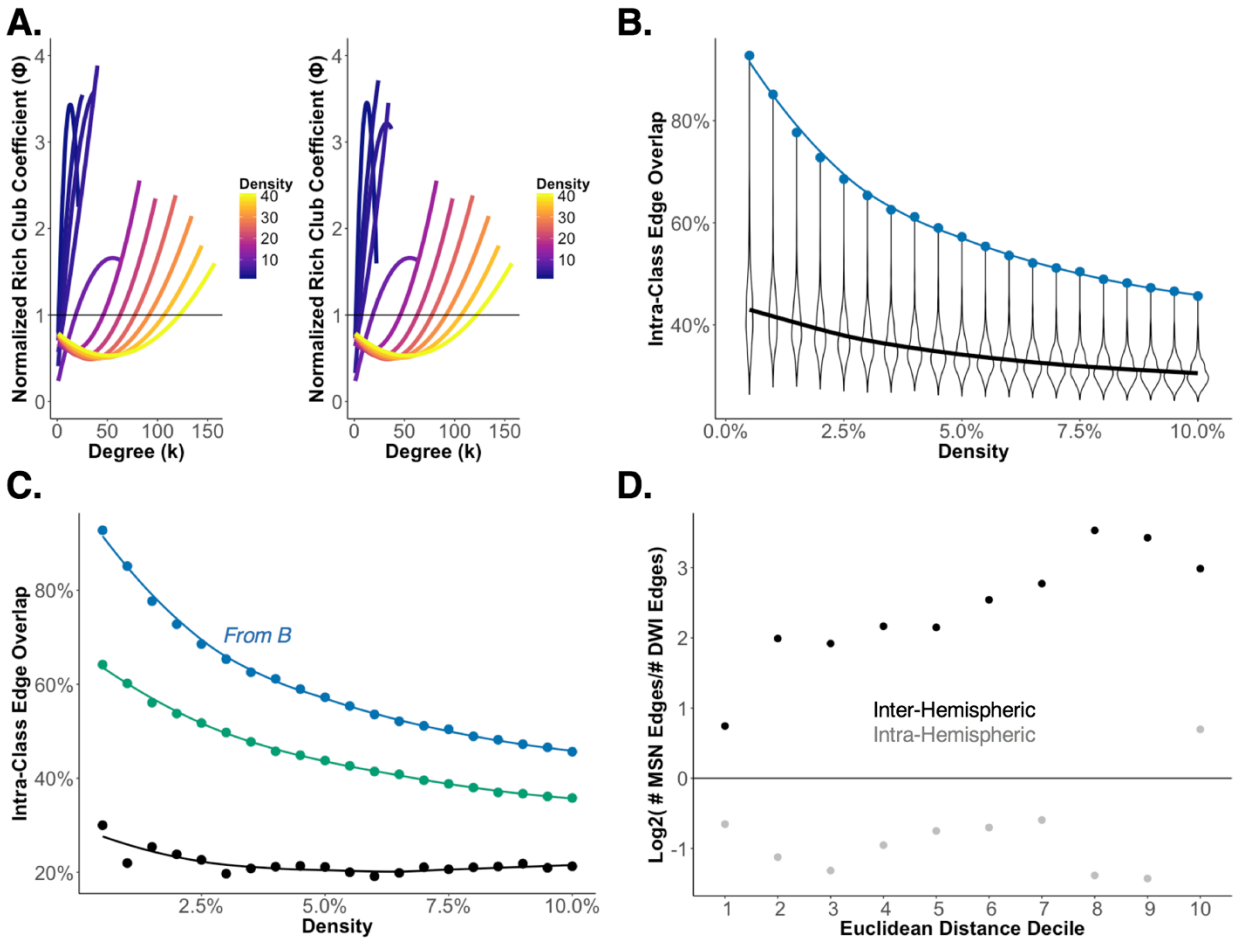

Figure S5. Stability of group NSPN MSN measurements and comparison with the group NSPN DWI network, Related to Figures 2 and 3. A) Rich club curves were computed for the group NSPN 10-feature MSN, plotted as the normalised rich club coefficient (phi) as a function of degree (k) for multiple connection densities (2, 3, 4, 5%; 10-40%, 5% intervals). A rich club is present in the group NSPN MSN at each of the connection densities for both binarised (left) and weighted (right) networks. **B)** At each connection density (0.5-10%, 0.5% intervals), the percent of intra-class overlap of the group NSPN MSN within the empirical cytoarchitectonic classes (blue) was greater than the intra-class overlap computed for 1000 pseudoparcellations (black). **C)** We chose use the edgewise average of the MD values of the streamlines for each individual network for our group NSPN DWI network (green) due to it having the greatest intra-class overlap (across connection densities) than that of the group DWI network computed using more complex averaging approaches (black; Mišić et al., 2015). **D)** Results of binomial (logistic) regression analysis modelling the presence versus absence of a detected edge, as a function of network type (group MSN or DWI, as constructed per Mišić et al. 2015), connection type (inter- vs. intra-hemispheric), and connection length (Euclidean length deciles) showed significant effects for network type (χ^2 = 107.328), connection type (χ^2 = 39.096), distance (χ^2 = 13212.262), and the interaction between network type, distance, and connection type (χ^2 = 110.383).

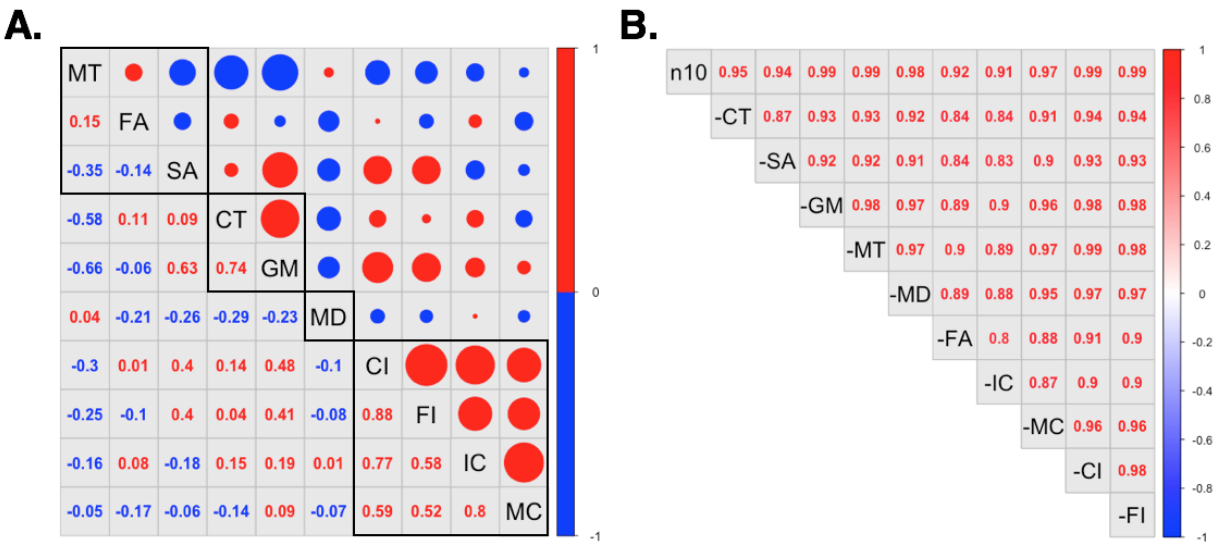

Figure S6. Properties of the cortical morphometric features, Related to Figures 1 and 2. A) The average correlation between the morphometric variables (in the primary NSPN cohort) was generated by calculating the correlation between the nodal feature estimates for each subject, and then averaging each correlation across subject. Outlines depicts groupings based on hierarchical clustering. **B)** Leave-one-feature-out analysis of the MSNs in the NSPN cohort. To evaluate the consistency of each subject's MSN, we computed the edgewise correlation between each subject's 10-feature MSN, and MSNs constructed leaving one feature out. The correlation plot shows the average correlation across subjects, and demonstrates high robustness of the morphometric similarity method to the removal of an individual feature.

Table S1.

Description	Pearson *r*			Spearman *ρ*		
	Mean	Min	Max	Mean	Min	Max
Nodal size vs. nodal similarity (people)	0.34	-0.37	0.78	0.35	-0.37	0.80
Nodal size vs. nodal similarity (nodes)	0.20	-0.18	0.51	0.22	-0.17	0.53
Nodal size vs. nodal similarity (people) – HCP parcellation	-0.05	-0.18	0.08	-0.60	-0.80	-0.12
Nodal size vs. nodal similarity (nodes) – HCP parcellation	0.18	-0.56	0.13	-0.17	-0.59	0.13
Nodal MAD vs. nodal size (MyConnectome)	0.05	N/A	N/A	0.04	N/A	N/A
Individual vs. group MSN (edges)	0.60	0.36	0.70	0.58	0.34	0.69
Individual vs. group MSN (nodes)	0.66	0.26	0.83	0.65	0.26	0.83
Group 10- vs. 5-feature (edges)	0.68	N/A	N/A	0.66	N/A	N/A
Group 10- vs. 5-feature (nodes)	0.91	N/A	N/A	0.91	N/A	N/A
Group MSN vs. gene expression (edges)	0.33	N/A	N/A	0.31	N/A	N/A
Group MSN vs. HSE gene expression	0.34	N/A	N/A	0.32	N/A	N/A
Group MSN vs. HSE gene co-expression	0.48	N/A	N/A	0.41	N/A	N/A
Group MSN vs. gene expression (all donors; edges)	0.79	0.63	0.90	0.75	0.55	0.87
Macaque group MSN vs. tract tracing	0.34	N/A	N/A	0.32	N/A	N/A
Macaque consensus vs. tract tracing	0.58	0.36	0.90	0.56	0.14	0.89
PLS1 scores vs. nodal size	-0.01	N/A	N/A	-0.05	N/A	N/A
PLS2 scores vs. nodal size	0.09	N/A	N/A	0.11	N/A	N/A

Table S1. Comparison of relational statistics computed using the Pearson and Spearman correlation, Related to Figures 1-6. All statistics remained consistent across both methods of correlation. The HCP parcellation refers to the one reported in Glasser et al., 2016.